Cooperativity-driven singularities in asymmetric exclusion

J. Stat. Mech. (2011) P06008

(http://iopscience.iop.org/1742-5468/2011/06/P06008)

Journal of Statistical Mechanics: Theory and Experiment
An IOP and SISSA journal

Cooperativity-driven singularities in asymmetric exclusion

Alan Gabel and S Redner

Center for Polymer Studies and Department of Physics, Boston University, Boston, MA 02215, USA
E-mail: agabel@bu.edu and redner@bu.edu

Received 18 May 2011
Accepted 24 May 2011
Published 9 June 2011

Online at stacks.iop.org/JSTAT/2011/P06008
doi:10.1088/1742-5468/2011/06/P06008

Abstract. We investigate the effect of cooperative interactions on the asymmetric exclusion process, which causes the particle velocity to be an increasing function of the density. Within a hydrodynamic theory, initial density upsteps and downsteps can evolve into: (a) shock waves, (b) continuous compression or rarefaction waves, or (c) a mixture of shocks and continuous waves. These unusual phenomena arise because of an inflection point in the current versus density relation. This anomaly leads to a group velocity that can be either an increasing or a decreasing function of the density on either side of the inflection point, a property that underlies these localized wave singularities.

Keywords: driven diffusive systems (theory), stochastic particle dynamics (theory), transport processes/heat transfer (theory)

ArXiv ePrint: 1101.5139

J. Stat. Mech. (2011) P06008

Contents

1. Introduction 2
2. The cooperative exclusion model 3
3. Density-profile dynamics 4
3.1. Shock/inverted shock 5
3.2. Continuous rarefaction/compression 6
3.3. Composite rarefaction/compression and shock 7
Acknowledgments 8
References 8

1. Introduction

The asymmetric exclusion process (ASEP) [1]–[5] represents an idealized description of transport in crowded one-dimensional systems, such as traffic [6]–[8], ionic conductors [9], and RNA transcription [10]. In the ASEP, each site is either vacant or occupied by a single particle that can hop at a fixed rate to a vacant right neighbor [1]–[4]. Although simply defined, this model has rich transport properties: for example, density heterogeneities can evolve into rarefaction or shock waves [4], while an open system, with input at one end and output at the other, exhibits a variety of phases as a function of the input/output rates [11]–[13].

A fundamental property of the ASEP is the relation $J(\rho) = \rho(1-\rho)$ between the current J and density ρ. Because each site is occupied by at most one particle, the average particle velocity $v = J/\rho$ is a decreasing function of the density. In this work, we investigate a cooperative exclusion (CE) model in which the velocity can increase with density. This cooperativity leads to unexpected features in the evolution of initial density heterogeneities. Such cooperativity occurs, for example, when ants emit pheromones that help guide fellow ants along a trail [14]. Another example is that of multiple buses that follow a fixed route. The leading bus picks up more passengers, so the next bus moves faster, which causes clustering of buses during peak travel times [15]. At the microscopic level, molecular motors can work together to pull a load that is too large for a single motor [16]. Cooperativity was even proposed as a basis for organic superconductors [17].

The notion of cooperative interactions that counterbalance the fundamental excluded-volume interaction is implicit in [7], as well as in [18, 19]. These latter publications investigated an exclusion model with a somewhat less stringent excluded-volume constraint than in ASEP. This weaker exclusion gives rise to an effective cooperativity and thereby to complex density profiles similar to what we find. As we shall argue, the existence of these complex profiles does not depend on detailed microscopic rules, but is rather a consequence of the underlying cooperative interactions between particles. When sufficiently strong, these interactions lead to an inflection point in the current–density curve; this feature is the minimum requirement for the complex density-profile dynamics.

doi:10.1088/1742-5468/2011/06/P06008

J. Stat. Mech. (2011) P06008

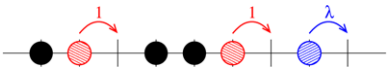

Figure 1. Cooperative exclusion. A 'pushed' particle (red)—one whose left neighbor is occupied—can hop to a vacant right neighbor with rate 1, while an isolated particle (blue) hops to a vacancy with rate λ.

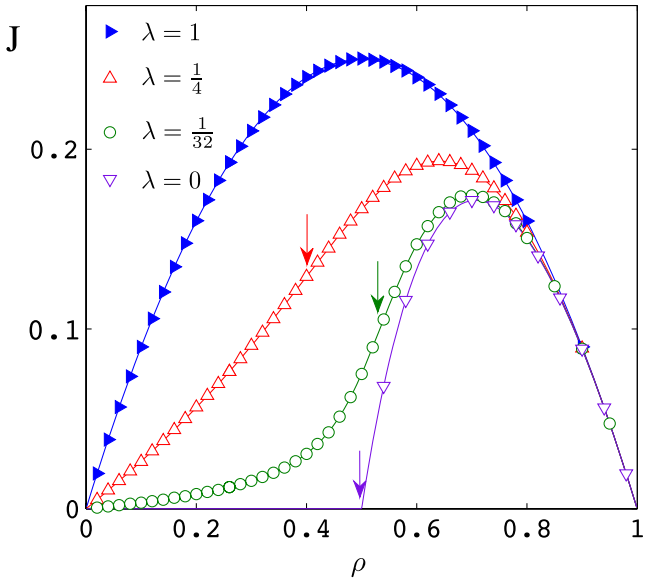

Figure 2. Steady-state current as a function of density in cooperative exclusion (CE). Data are based on 10^2 realizations with $L = 10^3$ up to $t = 10^4$. The solid curves are given by equation (2). Arrows indicate the locations of the inflection points.

2. The cooperative exclusion model

In the CE model, a particle can hop to its vacant right neighbor at a rate r that depends on the occupancy of the previous site (figure 1):

$$r = \begin{cases} 1 & \text{previous site occupied,} \\ \lambda & \text{previous site vacant,} \end{cases}$$

with $0 \leq \lambda \leq 1$. When $\lambda = 1$, the standard ASEP is recovered, while $\lambda = 0$ corresponds to facilitated asymmetric exclusion [20], in which the left neighbor of a particle must be occupied for the particle to hop to a vacancy on the right. We pictorially view this restriction as a particle requiring a "push" from its left neighbor to hop. This facilitation causes an unexpected discontinuity in a rarefaction wave in the ASEP [21]. More strikingly, we will show that cooperativity leads to shock and rarefaction waves that can be continuous, discontinuous, or a mixture of the two.

These unusual features arise in CE when $0 < \lambda < \frac{1}{2}$, where an inflection point in $J(\rho)$ occurs at $\rho = \rho_{\rm I}$ (figure 2). For $\rho < \rho_{\rm I}$, cooperativity dominates, and J grows superlinearly in ρ. At higher densities, excluded-volume interactions dominate, so J grows sublinearly

J. Stat. Mech. (2011) P06008

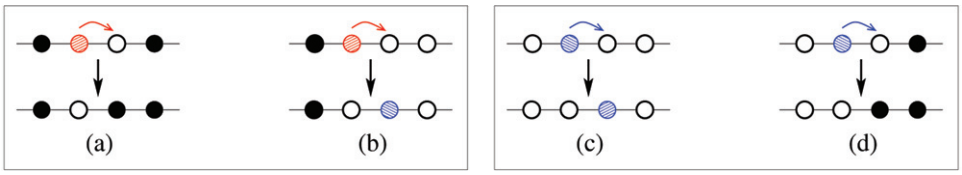

Figure 3. Left: hopping of a pushed (red) particle where the number of vacancy pairs is (a) preserved or (b) decreases. Right: hopping of an isolated (blue) particle where the number of vacancy pairs is (c) preserved or (b) increases.

and ultimately decreases to zero. Correspondingly, the group velocity changes from an increasing to a decreasing function of density ρ as ρ passes through $\rho_{\rm I}$.

A configuration of N particles on a ring of length L is specified by the occupation numbers $\{n_1, \ldots, n_L\}$, subject to particle conservation: $\sum_i n_i = N$; here n_i equals 1 if i is occupied and equals 0 otherwise. A crucial feature of CE is that the probability for any steady-state configuration is a decreasing function of the number k of adjacent vacancies: $k \equiv \sum_{i=1}^{L}(1-n_i)(1-n_{i+1})$, with $n_{L+1} = n_1$. To understand how the configurational probabilities depend on k, we observe that the hopping of a pushed particle (whose left neighbor is occupied) either preserves or decreases the number of adjacent vacancies k (left side of figure 3). Conversely, the hopping of an isolated particle either preserves or increases k (right side of figure 3). Since pushed particle hopping events occur at a higher rate, configurations with fewer adjacent vacancies are statistically more probable.

We now exploit the work of Antal and Schütz [7] who investigated a dual model in which next-nearest neighbor cooperative interactions pull a particle ahead, in distinction to the pushing of particles from behind in CE. By the mapping particles $\leftrightarrow$ holes, the CE and the Antal–Schütz models give the same probability distribution P_k for a configuration with k adjacent vacancies [7]:

$$P_k = \frac{\lambda^k}{Z(\lambda)}, \tag{1}$$

where $Z(\lambda)$ is a normalization constant. Since $\lambda < 1$, configurations with fewer adjacent vacancies are more probable. Following [7], the steady-state current is

$$J = (1-\rho)\left[1 + \frac{\sqrt{1-4(1-\lambda)\rho(1-\rho)}-1}{2(1-\lambda)\rho}\right] \tag{2}$$

in the $L \to \infty$ limit. The salient feature is that J has an inflection point at a density $\rho_{\rm I}$ for $\lambda < \frac{1}{2}$ (figure 2). We henceforth restrict our analysis to this domain and determine the unusual consequences of this inflection point on the dynamics of initial density steps.

3. Density-profile dynamics

In a hydrodynamic description, the particle satisfies the continuity equation $\rho_t + J_x = 0$. By the chain rule, we rewrite the second term as $J_\rho\, \rho_x$, from which the group velocity $u = J_\rho$. Here the subscripts t, x, ρ denote partial differentiation. The crucial feature is the inflection point in $J(\rho)$, so the group velocity can be either increasing or decreasing in ρ. We now employ the steady-state current (2) to determine the evolution of an initial

J. Stat. Mech. (2011) P06008

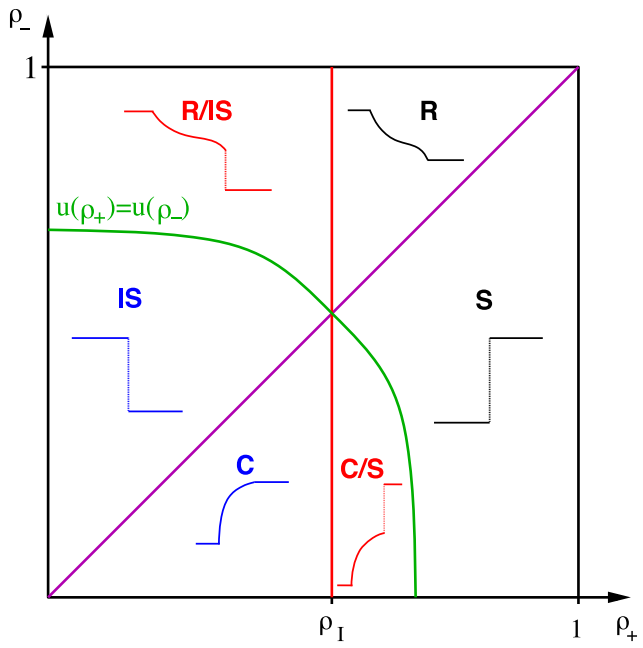

Figure 4. Phase diagram of the CE model for an initial density step (ρ_-, ρ_+), with ρ_I the inflection point in $J(\rho)$. A typical density profile $\rho(z)$ is sketched for each of the six regions: (R/IS) rarefaction/inverted shock, (R) continuous rarefaction, (S) shock, (C/S) compression/shock, (C) continuous compression, (IS) inverted shock.

density heterogeneity on length and time scales large compared to microscopic scales for the step initial condition

$$\rho(x, t = 0) = \begin{cases} \rho_- & x \leq 0, \\ \rho_+ & x > 0. \end{cases} \tag{3}$$

As sketched in figure 4, the difference of the group velocities to the right and left of the step determines whether a continuous, discontinuous, or a composite density profile emerges.

It is worth noting that similar results for density profiles were obtained for an asymmetric exclusion process with another form of cooperative interaction [18, 19]. In that work, the same qualitative phase diagram as in figure 4 was obtained, despite the rather different natures of the microscopic interactions in their model. This similarity in long-time behavior arises because our main results apply for any asymmetric exclusion process with sufficiently strong cooperative interactions, as indicated by an inflection point in $J(\rho)$.

3.1. Shock/inverted shock

A propagating shock wave arises whenever the group velocity on the left exceeds that on the right, $u(\rho_-) > u(\rho_+)$. Qualitatively, the faster moving particles catch up to slower particles on the right and pile up in a shock wave, just as freely moving cars suddenly slow down upon approaching a traffic jam. In the conventional ASEP, all upsteps evolve into

J. Stat. Mech. (2011) P06008

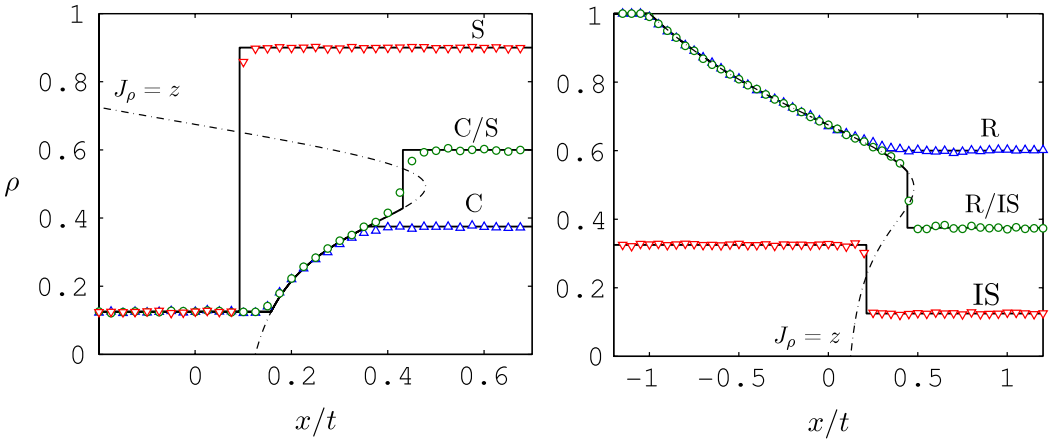

Figure 5. Left: evolution of an upstep for $\lambda = \frac{1}{8}$: (C) continuous compression wave for $\rho_- = \frac{1}{8}$, $\rho_+ = \frac{3}{8}$; (C/S) composite compression/shock for $\rho_- = \frac{1}{8}$, $\rho_+ = \frac{6}{10}$; (S) shock for $\rho_- = \frac{1}{8}$, $\rho_+ = \frac{9}{10}$. Right: evolution of a downstep for $\lambda = \frac{1}{8}$: (R) continuous rarefaction for $\rho_- = 1$, $\rho_+ = \frac{6}{10}$; (R/IS) composite rarefaction/inverted shock for $\rho_- = 1$, $\rho_+ = \frac{3}{8}$; (IS) inverted shock for $\rho_- = 0.325$, $\rho_+ = \frac{1}{8}$. The dashed line is the locus $J_\rho = z$ and the solid black curves are analytic predictions. Simulations are based on 10^3 realizations up to $t = 4 \times 10^3$.

a shock (S) wave. For the CE, in contrast, only upsteps where both initial densities are above the inflection point, $\rho_I < \rho_- < \rho_+$, evolve into shocks (figure 5). Here, exclusion is sufficiently strong that the group velocity is a decreasing function of density. Strikingly, a propagating shock wave also emerges from a downstep in CE when the initial densities are both below the inflection point, $\rho_I > \rho_- > \rho_+$. In this regime, $J_{\rho\rho} = u_\rho > 0$; that is, cooperativity is sufficiently strong that particles in the high-density region on the left have a greater group velocity and therefore pile up at the interface. We term this singularity an inverted shock (IS) (figure 5).

For both shocks and inverted shocks, the density is given by the traveling wave profile $\rho = \rho(x-ct)$. We obtain the shock speed c by equating the net flux into a large region that includes the shock, $J(\rho_+) - J(\rho_-)$, with the change in the number of particles, $c(\rho_+ - \rho_-)$, in this region [22] to obtain the standard expression $c = [J(\rho_+) - J(\rho_-)][\rho_+ - \rho_-]$; this holds for both conventional and inverted shocks.

3.2. Continuous rarefaction/compression

A density step gradually smooths out when the group velocity to the left is less than that on the right, $u(\rho_-) < u(\rho_+)$. Here the faster particles on the right leave open space for the slower particles, which is similar to the case of a cluster of stopped cars that slowly spreads out after a stoplight turns green. In ASEP, a downstep always evolves to a continuous rarefaction (R) wave. This continuous rarefaction also occurs in CE when both initial densities are above the inflection point, $\rho_- > \rho_+ > \rho_I$. At these high densities, exclusion dominates, as in the ASEP, which causes the group velocity to decrease with density.

In striking contrast to the ASEP case, an upstep can continuously smooth out in CE when the initial densities are below the inflection point, $\rho_- < \rho_+ < \rho_I$. In this regime,

J. Stat. Mech. (2011) P06008

cooperativity is sufficiently strong that particles in the high-density region on the right move faster than those on the left. Thus instead of a shock wave, a continuous compression (C) wave develops (figure 5). We determine the density profile by assuming that it is a function of the scaled variable $z = x/t$. Substituting $\rho(x,t) = \rho(z)$ into the continuity equation gives $-z\rho_z + J_\rho\,\rho_z = 0$. Thus the profile consists either of constant-density segments ($\rho_z = 0$) or else $z = J_\rho$. Matching these solutions gives [5, 21]

$$\rho(z) = \begin{cases} \rho_- & z < z_-, \\ I(z) & z_- \le z \le z_+, \\ \rho_+ & z > z_+, \end{cases} \tag{4}$$

where $I(z)$ is the inverse function of $z = J_\rho$. For a continuous profile, the cutoffs z_- and z_+ are determined by matching the interior solution $I(z)$ with the asymptotic solutions: $I(z_\pm) = \rho_\pm$ or equivalently, $z_\pm = J_\rho(\rho_\pm)$.

3.3. Composite rarefaction/compression and shock

In CE, a continuous rarefaction or compression wave can coexist with a shock wave. This phenomenon occurs when the group velocity on the left is initially less than that on the right but also with the constraint that the initial densities lie on either side of the inflection point. Consequently one side of the step is in the exclusion-dominated regime and the other is in the cooperativity-dominated regime, or vice versa. In particular, a composite rarefaction/inverted shock (R/IS) wave emerges from a downstep when $\rho_- > \rho_{\rm I} > \rho_+$, so $u(\rho_-) < u(\rho_+)$. As in the case of the continuous rarefaction wave, the downstep begins to smooth out from the rear. Consequently, cooperative interactions become more important as the density at the leading edge of this rarefaction decreases. Eventually this leading density reaches the point where the particle speed matches that at the bottom of the downstep and the rarefaction front terminates in an inverted shock.

Correspondingly, an upstep can evolve to a compression wave with a leading shock when the densities satisfy $\rho_- < \rho_{\rm I} < \rho_+$ and $u(\rho_-) < u(\rho_+)$. In this case, the leading particles initially race ahead, leaving behind a profile where the density increases with x. However, this increase cannot be continuous because eventually a point is reached where the speed at the front of this continuous wave matches that of the top of the upstep. After this point, a pile-up occurs and a shock wave forms. We call this profile a composite compression/shock (C/S) wave (figure 5).

The functional forms of the composite rarefaction/inverted shock and composite compression/shock profiles are still given by equation (4), but the criteria for determining the cutoffs $z_\pm$ are now slightly more involved than for continuous profiles. The location of the left cutoff, z_-, is again determined by continuity, namely, $I(z_-) = \rho_-$ or, alternatively, $z_- = J_\rho(\rho_-)$. To determine the right cutoff z_+, note that in a small spatial region that includes the leading-edge discontinuity, the density profile is just that of a shock or inverted shock wave. Thus the equation for the shock speed is

$$z_+ = \frac{J(q_+) - J(\rho_+)}{q_+ - \rho_+}, \tag{5}$$

where $q_+ \equiv I(z_+)$ is the density just to the left of the discontinuity. (Note also that $z_+ = J_\rho(q_+)$ by definition.) To justify (5), we use the conservation condition that the

J. Stat. Mech. (2011) P06008

particle number in $[z_-, z_+]$ equals the initial number plus the net flux into this region:

$$\int_{z_-}^{z_+} I(z)\,\mathrm{d}z = -\rho_- z_- + \rho_+ z_+ - J(\rho_+) + J(\rho_-). \tag{6}$$

We recast this expression as (5), by making the variable change $z = J_\rho(\rho)$ and using $I(J_\rho(\rho)) = \rho$ to write the integral as $\int_{\rho_-}^{q_+} \rho\, J_{\rho\rho}\,\mathrm{d}\rho$; the integration can now be performed by parts. The resulting expression readily simplifies to (5).

In summary, a diversity of wave singularities arise in asymmetric exclusion with sufficiently strong cooperativity. The minimum requirement for these phenomena is an inflection point in the current–density relation $J(\rho)$. This inflection point leads to a group velocity that is an increasing function of density for $\rho < \rho_\mathrm{I}$, a dependence opposite to that in the conventional ASEP. The resulting non-monotonic density dependence of the velocity causes an initial density upstep or downstep to evolve to: shock/inverted shocks, continuous rarefaction/compression waves, or a composite profile with both continuous and discontinuous elements.

Acknowledgments

We thank Martin Schmaltz for asking an oral exam question that helped spark this work and Paul Krapivsky for helpful discussions. We also thank the referee for informing us about [18, 19]. Finally, we gratefully acknowledge financial support from NSF grant DMR-0906504.

References

[1] Schmittmann B and Zia R K P, 1995 *Phase Transitions and Critical Phenomena* vol 17, ed C Domb and J L Lebowitz (London: Academic)
[2] Derrida B, 1998 *Phys. Rep.* **301** 65
Derrida B, 2007 *J. Stat. Mech.* P07023
[3] Schütz G, 2000 *Phase Transitions and Critical Phenomena* vol 19, ed C Domb and J L Lebowitz (London: Academic)
[4] Blythe R A and Evans M R, 2007 *J. Phys. A: Math. Theor.* **40** R333
[5] Krapivsky P L, Redner S and Ben-Naim E, 2010 *A Kinetic View of Statistical Physics* (Cambridge: Cambridge University Press)
[6] Popkov V and Schütz G M, 1999 *Europhys. Lett.* **48** 257
[7] Antal T and Schütz G M, 2000 *Phys. Rev.* E **62** 83
[8] Schadschneider A, Chowdhury D and Nishinari K, 2010 *Stochastic Transport in Complex Systems: From Molecules to Vehicles* (Amsterdam: Elsevier)
[9] Richards P M, 1977 *Phys. Rev.* B **16** 1393
[10] MacDonald C T, Gibbs J H and Pipkin A C, 1968 *Biopolymers* **6** 1
MacDonald C T and Gibbs J H, 1969 *Biopolymers* **7** 707
[11] Krug J, 1991 *Phys. Rev. Lett.* **67** 1882
[12] Derrida B, Domany E and Mukamel D, 1992 *J. Stat. Phys.* **69** 667
[13] Schütz G M and Domany E, 1993 *J. Stat. Phys.* **72** 277
[14] Burd M, Archer D, Aranwela N and Stradling D J, 2002 *Am. Nat.* **159** 283
[15] O'Loan O J, Evans M R and Cates M E, 1998 *Phys. Rev.* E **58** 1404
[16] Chowdhury D, 2006 *Physica* A **372** 84
[17] Little W A, 1964 *Phys. Rev. Lett.* **134** A1416
Little W A, 1965 *Sci. Am.* **212** 21
[18] Freire M V, Guiiol H, Ravishankar K and Saada E, 2002 *Bull. Braz. Math. Soc.* **33** 319
[19] Bahadoran C, Guiol H, Ravishankar K and Saada E, 2002 *Stoch. Process. Appl.* **99** 1
[20] Basu U and Mohanty P K, 2009 *Phys. Rev.* E **79** 041143
[21] Gabel A, Krapivsky P L and Redner S, 2010 *Phys. Rev. Lett.* **105** 210603
[22] Whitham G B, 1974 *Linear and Nonlinear Waves* (New York: Wiley)

J. Stat. Mech. (2011) P06008